

# Journal of Astronomical Telescopes, Instruments, and Systems

AstronomicalTelescopes.SPIEDigitalLibrary.org

## Table-top soft x-ray polarimetry setup with rotatable linearly polarized light source

Wenbin Li  
Yujie Xing  
Yue Yu  
Mingwu Wen  
Chun Xie  
Qiushi Huang  
Zhong Zhang  
Shengzhen Yi  
Zhanshan Wang

**SPIE.**

Wenbin Li, Yujie Xing, Yue Yu, Mingwu Wen, Chun Xie, Qiushi Huang, Zhong Zhang, Shengzhen Yi, Zhanshan Wang, "Table-top soft x-ray polarimetry setup with rotatable linearly polarized light source," *J. Astron. Telesc. Instrum. Syst.* **5**(1), 019003 (2019), doi: 10.1117/1.JATIS.5.1.019003.

# Table-top soft x-ray polarimetry setup with rotatable linearly polarized light source

Wenbin Li,<sup>a,b</sup> Yujie Xing,<sup>a,b</sup> Yue Yu,<sup>a,b</sup> Mingwu Wen,<sup>a,b</sup> Chun Xie,<sup>c</sup> Qiushi Huang,<sup>a,b</sup> Zhong Zhang,<sup>a,b</sup> Shengzhen Yi,<sup>a,b</sup> and Zhanshan Wang<sup>a,b,\*</sup>

<sup>a</sup>MOE Key Laboratory of Advanced Micro-Structured Materials, Shanghai, China

<sup>b</sup>Tongji University, Institute of Precision Optical Engineering, School of Physics Science and Engineering, Shanghai, China

<sup>c</sup>Tongji University, Sino-German College of Applied Sciences, Shanghai, China

**Abstract.** A table-top soft x-ray polarimetry setup has been developed at the Institute of Precision Optical Engineering for characterizing the polarization properties of mirrors designed for the lightweight asymmetry and magnetism probe project. Based on a Co/C multilayer polarizer mirror, linearly polarized soft x-rays were generated at a wavelength of 4.48 nm, which could be rotated around the beam-propagation direction by using a differentially pumped rotary feedthrough. The setup design and the alignment method are described in detail. The capabilities of this spectrometer were demonstrated through a polarization test on a twin Co/C multilayer polarizer sample, and the results agree well with the expected sine wave. © The Authors. Published by SPIE under a Creative Commons Attribution 4.0 Unported License. Distribution or reproduction of this work in whole or in part requires full attribution of the original publication, including its DOI. [DOI: [10.1117/1.JATIS.5.1.019003](https://doi.org/10.1117/1.JATIS.5.1.019003)]

Keywords: polarimeter; soft x-rays; Co/C multilayer; polarization.

Paper 18078 received Oct. 6, 2018; accepted for publication Jan. 23, 2019; published online Feb. 7, 2019.

## 1 Introduction

Polarization, a fundamental property of electromagnetic radiation, is critical for exploring extreme astrophysical phenomena. The detection and analysis of x-ray polarization can help reveal the structures of active galactic nuclei, jet x-ray emission mechanisms, and so on.<sup>1,2</sup> In the soft x-ray energy region below 1 keV, polarimeter instruments based on multilayer mirrors have been proposed for astronomical observations, such as the polarimeter for low-energy x-ray astrophysical sources, which uses a lateral-gradient multilayer polarizer,<sup>3</sup> and a simple soft x-ray polarimeter design using periodic multilayer polarizers.<sup>4</sup>

In China, a microsatellite mission concept called lightweight asymmetry and magnetism probe (LAMP) has been proposed to measure the polarization of monochromatic soft x-rays at ~250 eV, key technology study is ongoing for this proposal.<sup>5</sup> According to the proposal, the LAMP instrument is planned to be constructed with 16 paraboloidal multilayer mirror sectors mounted circularly around the focal-plane detectors. The multilayer mirrors used in LAMP should provide a sufficiently high reflectivity near the Brewster's angle of 45 deg and simultaneously achieve a high polarization efficiency between s- and p-polarized lights ( $R_s/R_p$ ).<sup>6,7</sup> Usually, the reflectivity and polarization efficiency of multilayer mirrors are accurately characterized using dedicated beamlines and spectrometers provided in synchrotron radiation facilities.<sup>8,9</sup> However, in such cases, it is necessary to apply for a scheduled beamtime in advance. Consequently, mirrors cannot be conveniently and routinely characterized immediately after fabrication. Therefore, a laboratory-based experimental setup is highly desired to characterize the polarization and reflectivity properties of mirror samples.

In the laboratory, many standalone reflectometers have been built for characterizing the optical properties of mirrors covering the energy region from ultraviolet to hard x-rays,<sup>10–12</sup> especially at 13.5 nm owing to strong demands for extreme-ultraviolet lithography.<sup>13,14</sup> However, as we know, few laboratory-based instruments have been built in the soft x-ray energy region for polarization characterization,<sup>15,16</sup> which requires a linearly polarized soft x-ray light source. For measuring the linear x-ray polarization over a soft x-ray energy range of 0.2 to 0.8 keV, Marshall et al.<sup>17</sup> developed a broadband soft x-ray polarimeter based on a lateral-gradient multilayer mirror and an x-ray grating. In order to perform preliminary tests on the polarization properties of mirrors for the LAMP project, a soft x-ray polarimetry setup was designed and constructed at the Institute of Precision Optical Engineering (IPOE). In this paper, the structure and performance of this setup are presented, including polarization measurement on a Co/C multilayer sample.

## 2 Soft X-Ray Polarimetry Setup

Figure 1 shows a schematic of the soft x-ray polarimetry setup, which consists mainly of three sections, namely a light-source chamber, transport beamline, and sample chamber. The light-source chamber is rotatable around the beam-propagation direction to generate a rotatable linearly polarized soft x-ray beam. The polarized light is transported from the source to the sample chamber through the beamline section. The polarization and reflectivity properties of the sample mirror are measured and characterized in the sample chamber. In the following, the structures and functions of these sections are presented in detail.

The light-source chamber includes a soft x-ray light tube, a multilayer polarizer mirror, a differentially pumped rotary feedthrough (DPRF), and a vacuum chamber. The soft x-ray light tube (Model 642, McPHERSON) was mounted on the chamber's flange orientated perpendicular to the beamline. Different anodes can be used in the light tube to generate unpolarized soft x-rays at different wavelengths. In the present experiment,

\*Address all correspondence to Zhanshan Wang, E-mail: [wangzs@tongji.edu.cn](mailto:wangzs@tongji.edu.cn)

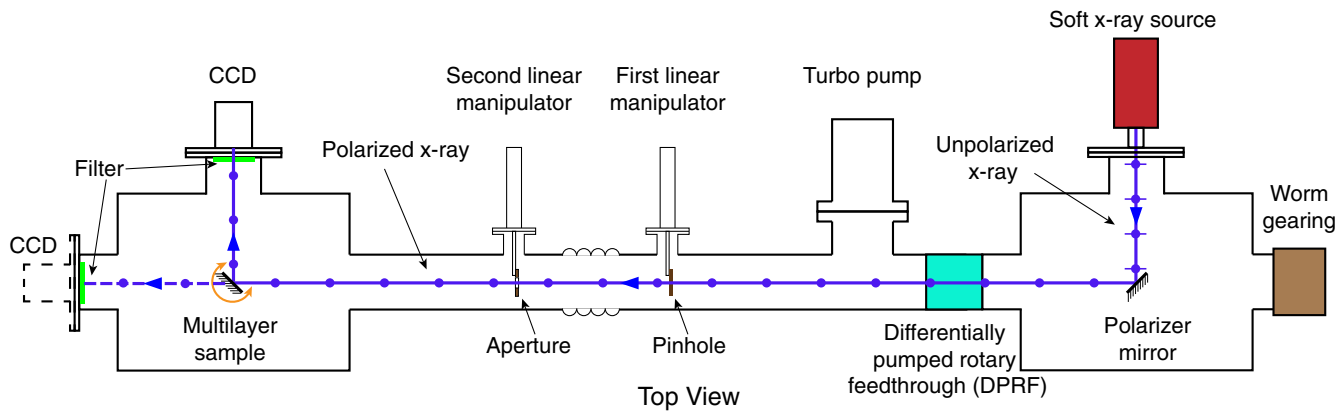


**Fig. 1** Schematic of the soft x-ray polarimetry setup. The dashed blue line represents the optical path for pinhole imaging and the polarized x-ray beam intensity detection experiment. The solid blue line represents the optical path for measuring the polarization and reflectivity properties of the multilayer sample.

a carbon anode was used to produce soft x-rays at 4.48 nm (277 eV) for testing. During the experiment, the source was operated at an anode voltage of 5 kV with a beam current of 0.4 mA, and the output of the unpolarized light was estimated to be  $4.7 \times 10^{11}$  photons/s/sr according to the user manual.<sup>18</sup>

For producing linearly polarized light, a periodic Co/C multilayer mirror was used as the x-ray polarizer. This polarizer, which consisted of 100 alternating layers of Co and C with layer thicknesses of  $d_{\text{Co}} = 1.28$  nm and  $d_{\text{C}} = 1.91$  nm, respectively, was fabricated at IPOE by using the reactive sputtering method with Ar + 6%N<sub>2</sub> as the working gas. The nominal reflectivity of this Co/C multilayer was estimated to be 0.09 for unpolarized light and 0.18 for s-polarized light at a working wavelength of 4.48 nm according to a simulation using IMD software,<sup>19</sup> in which the bulk densities of layer materials and an interface width of 0.57 nm were used based on previous experimental results.<sup>7</sup> The polarizer mirror was mounted on a dual-axis mirror holder placed at the center of the light-source chamber. Linearly polarized light was generated by reflecting the incident unpolarized light with the polarizer at the Brewster angle of  $\sim 45$  deg. A DPRF connected the outlet flange of the light-source chamber with the transport beamline. Additionally, a worm gearing was mounted on another flange opposite to the rotary feedthrough, as shown in Fig. 1. Based on the DPRF and the worm gearing, the light-source chamber can be rotated manually around the central axis of the chamber from 0 deg to 360 deg with an angular accuracy of 1 deg. Therefore, linearly polarized soft x-ray light was generated with the polarization vector rotatable in the plane perpendicular to the beam direction. During rotation, the pressure of the vacuum chamber varied within the range of  $\pm 1 \times 10^{-4}$  Pa, which is sufficiently safe even for the current-carrying filament in the light tube.

As shown in Fig. 1, an extensible transport beamline was used to connect the light source chamber and sample chamber. A turbo pump, which was mounted on a side flange of the beamline pipe near the light-source chamber, was used to pump the whole system down to a base pressure of  $\sim 3 \times 10^{-4}$  Pa. Two linear manipulators were installed on the beamline pipe. For the first manipulator, one pinhole was mounted on the shaft for the pinhole experiment, as described in the following section. For the second manipulator, a collimating aperture with dimensions of 2 mm  $\times$  2 mm was mounted on the shaft, which could be moved down to the optical path to limit the

incident-beam divergence. In the present setup, the distance from the light source to the aperture was  $\sim 1.8$  m, and the distance from the aperture to the detector was  $\sim 0.8$  m. For testing the polarization performance of this setup, a twin Co/C multilayer sample was positioned at the center of the sample chamber. A soft x-ray charge-coupled device (CCD) detector (Princeton Instruments, PIXIS-XO:1024B) was used to measure the incident or reflected beam intensity. When the CCD detector was mounted on the flange toward the polarizer directly, as shown in Fig. 1, the incident beam intensity of the linearly polarized light can be measured directly by removing the sample. Alternatively, when the detector was mounted on the other flange perpendicular to the optical axis, the intensity of the beam reflected from the sample could be measured. For preventing visible light from entering the detector, a 100-nm-thick Al filter coated on a 500-nm-thick parylene-N (C<sub>8</sub>H<sub>8</sub>) membrane was placed immediately in front of the CCD detector. The transmissivity of the filter is  $\sim 0.40$  for radiation at 4.48 nm and nearly zero for visible light. The polarization properties of the multilayer mirror can be characterized by using this setup.

### 3 Alignment of the Polarimetry Setup and Experimental Results

#### 3.1 Alignment of the Polarimetry Setup

The most important task for alignment is to find the rotation axis of the light-source chamber and set it as the optical axis of the beamline. For this purpose, a small, compact red laser mounted on a multiaxis holder was first placed inside the light-source chamber near the worm gearing and pointed through the aperture to the sample chamber, as shown in Fig. 2. By carefully adjusting the multiaxis holder, the red laser spot, which was monitored  $\sim 3$  m away from the source, shifted within  $\pm 1$  mm when rotating the light-source chamber. This laser beam path was then considered as the rotation axis and the optical axis. Adjacent to this red laser, a compact green laser was installed at the left side outside the sample chamber and pointed along the optical axis toward the source chamber. The green laser beam was adjusted to be in alignment with the red laser beam along the whole optical axis.

After setting the optical axis, the polarizer mirror was set at a working angle of 45 deg with the aid of a right-angle prism and a plane mirror. The right-angle prism was placed at the center of

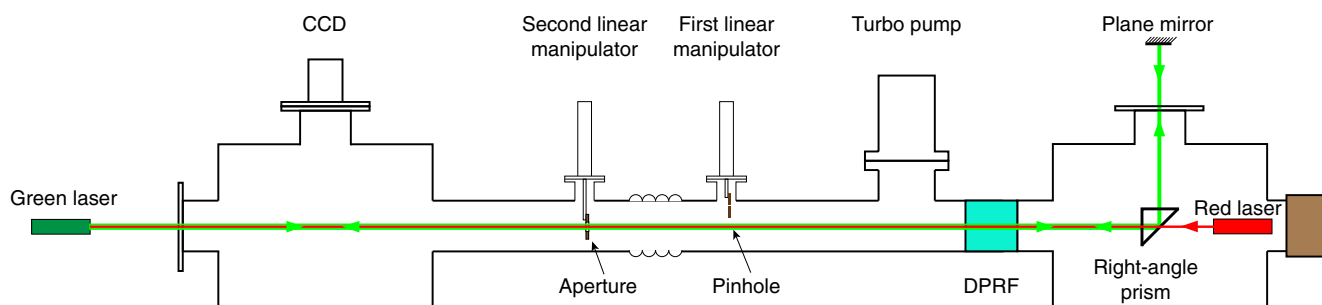


Fig. 2 Schematic of the alignment method for the polarimetry setup.

the light-source chamber, and the prism's leg face was adjusted to be perpendicular to the incident green laser beam. Therefore, the angle between the incident and exit green laser beam was precisely 90 deg with an accuracy of  $\pm 30''$ , which was determined by the angle tolerance of the prism. The exit green beam illuminated the plane mirror placed behind the mounting flange for the x-ray light tube. By adjusting the plane mirror's holder, the green beam reflected from the plane mirror propagated along the path in the opposite direction to the incoming beam and returned to the green laser emitter. Finally, the right-angle prism was replaced by the Co/C multilayer polarizer, and the polarizer holder was carefully adjusted to ensure that the green laser beam reflected by the plane mirror returned to the laser emitter along the same path. After positioning the polarizer mirror, a soft x-ray light tube was mounted on the flange to ensure that the green laser pointed to the anode center.

In the sample chamber, a twin Co/C multilayer was used as the sample mirror and attached to a dual-axis mirror holder. The mirror holder was mounted on a rotary manipulator, which is not shown in Figs. 1 or 2. The sample mirror was first rotated to be perpendicular to the green laser beam. Then, the mirror holder was adjusted to reflect the green laser back to the emitter. Finally, the rotary manipulator was rotated clockwise by 135 deg to set the incidence angle at 45 deg. The angular resolution of the rotatable manipulator was  $\sim 0.1$  deg. The soft x-ray beam reflected from the sample mirror was detected by the CCD detector oriented perpendicular to the optical axis, as shown in Fig. 1.

### 3.2 Divergence and Stability of X-Ray Beam

In this polarimetry setup, the light-beam divergence depends on the aperture dimensions, distance between the source and aperture, and spot size of the light source. Because the aperture size and distance were known, the spot size of the light source was measured using a pinhole imaging method in this experiment for estimating the beam divergence. As shown in Fig. 1, a 50- $\mu\text{m}$ -diameter pinhole was placed on the shaft of the first linear manipulator. The CCD detector was oriented directly toward the polarizer mirror. The aperture and multilayer sample were also removed without blocking the incident beam. The distance between the pinhole and light source was  $\sim 1.3$  m, which was roughly the same as the image distance from the pinhole to the CCD detector. Therefore, the amplification factor of the pinhole imaging is  $\sim 1$ .

The pinhole image of the soft x-ray light source after exposure for 20 s is shown in Fig. 3(a), in which the light source was operated at a voltage of 5 kV and the x-ray beam current was 0.4 mA. Figures 3(b) and 3(c) show the horizontal and vertical

projection data of the pinhole image, respectively. By fitting the experimental data with Gaussian profiles and taking account of the CCD pixel size of 13  $\mu\text{m}$ , the diameter of the x-ray spot was determined to be  $\sim 0.43$  mm (full width at half maximum; FWHM). According to the dimensions of the x-ray light source, we set up a simulation model for this optical system by using Lighttools software. Based on Monte-Carlo ray-tracing simulation results, the soft x-ray light-beam divergence was determined to be  $\sim 0.08$  deg (FWHM), which is much less than the angular bandwidth (FWHM  $\approx 0.7$  deg) of the curve of reflectivity as a function of incidence angle for the Co/C multilayer mirror.

For polarimetry measurement, it is quite important to have a stable beam during rotation of the light-source chamber. After alignment, the incident polarized beam intensity was measured using the CCD detector mounted on the flange oriented toward the polarizer mirror. The pinhole was moved out of the optical path, and the collimating square aperture was used to reduce the beam divergence. In this measurement, the light-source chamber was rotated from 0 deg to 360 deg in steps of 10 deg. The voltage and beam current were set to have the same values as in the pinhole image experiment, and the CCD acquisition time was 30 s for each image at each step. The acquired image has a square shape similar to the aperture, which is not given here. Figure 4(a) shows the averaged CCD count rate per pixel as a function of the rotation angle. It is found that the intensity variation of the polarized x-ray beam was about 4.5% (relative root mean square error; RRMSE) during rotation of the light-source chamber. In the measurement, the image position was also found to be shifted in the horizontal and vertical directions when changing the rotation angle. The relative position shifts are shown in Fig. 4(b). The x-ray spot position shifted within  $\pm 0.28$  mm in the horizontal direction and  $\pm 0.55$  mm in the vertical direction, and the shifts are smaller than the spot size of  $\sim 2$  mm  $\times$  2 mm. These results demonstrate that the intensity and position stability of the rotatable polarized x-ray source are suitable for the polarimetry experiment.

### 3.3 X-Ray Polarimetry Measurement

To test whether this system can generate 100% linearly polarized light, an x-ray polarization detection experiment was performed on a twin Co/C multilayer sample. The multilayer sample was oriented at 45 deg with respect to the incident x-ray beam. The CCD detector was placed at the horizontal plane and oriented perpendicular to the beamline, which means x-ray photons with a polarization vector perpendicular to the horizontal plane will be reflected by the multilayer and enter the detector. The voltage and beam current of the x-ray

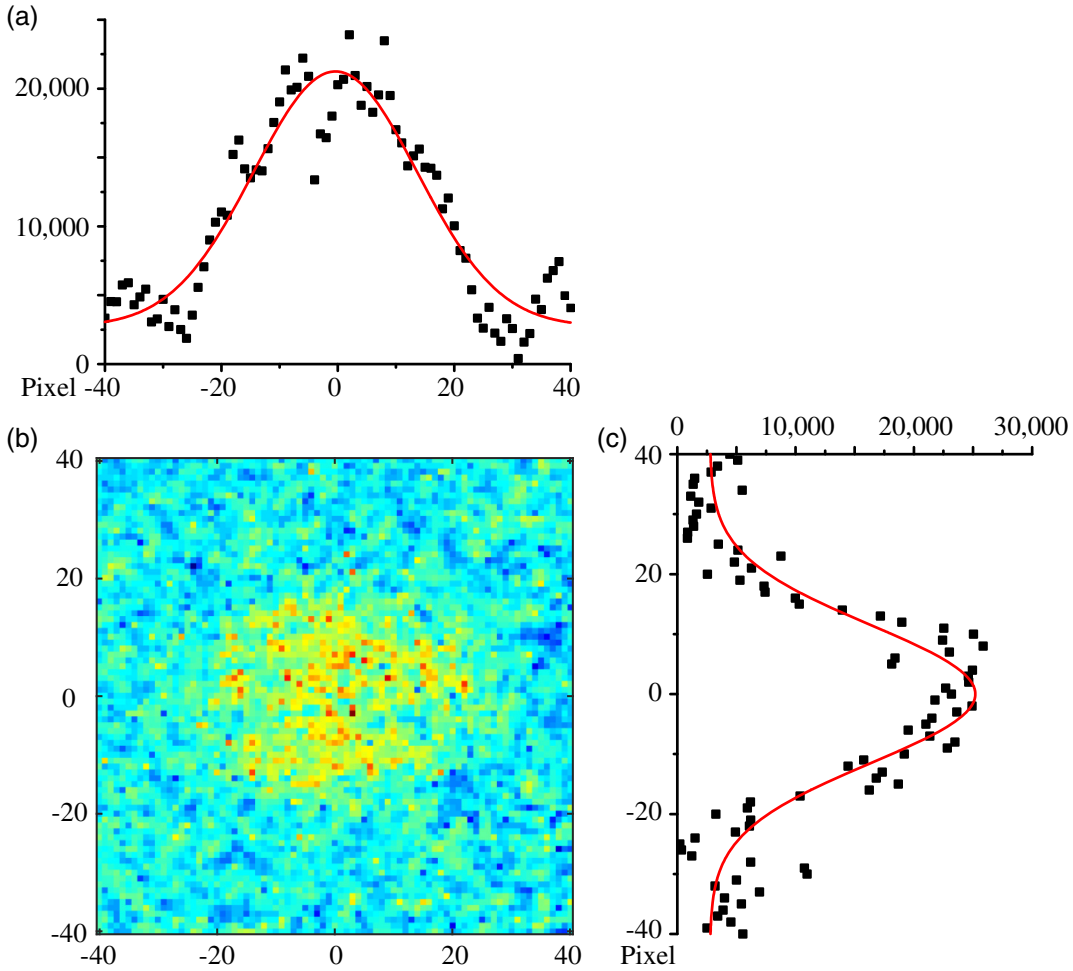


**Fig. 3** X-ray pinhole imaging experiment for the light source after alignment. (a) Horizontal projection data of the pinhole image and its fitting curve with a Gaussian profile. (b) Extracted CCD image having  $80 \times 80$  pixels. (c) Vertical projection data of the pinhole image and its fitting curve with a Gaussian profile.

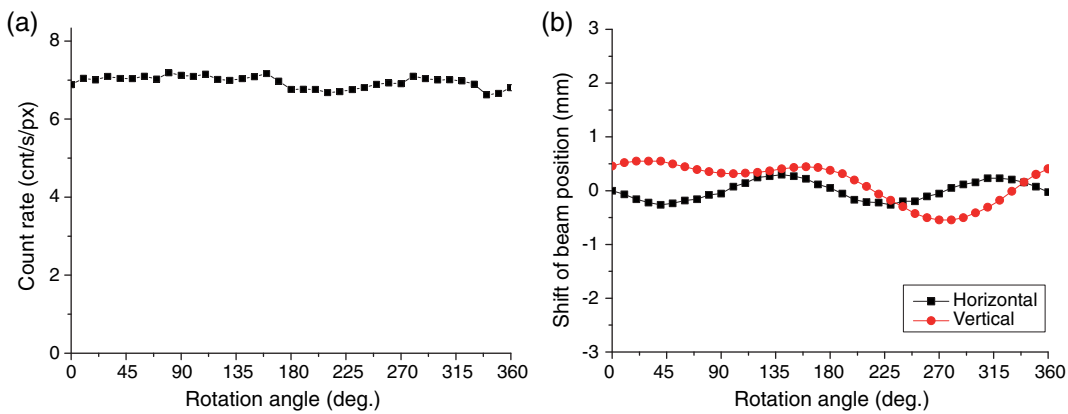


**Fig. 4** (a) Averaged CCD count rate per pixel and (b) relative beam position shifts as functions of the rotation angle.

source were the same as those used in the stability experiment. For the polarimetry experiment, the CCD detector acquired an image for 120-s exposures at each angle when rotating the light-source chamber from 0 deg to 360 deg in steps of 10 deg. Figure 5(a) shows the averaged count rate per pixel as a function

of the rotation angle, where a rotation angle of 0 deg (180 deg) indicates a polarization vector perpendicular to the plane of incidence (horizontal plane). As expected, the experimental data were well fitted by a sine wave, as shown by the red solid curve in Fig. 5. At rotation angles of 90 deg and 270 deg,

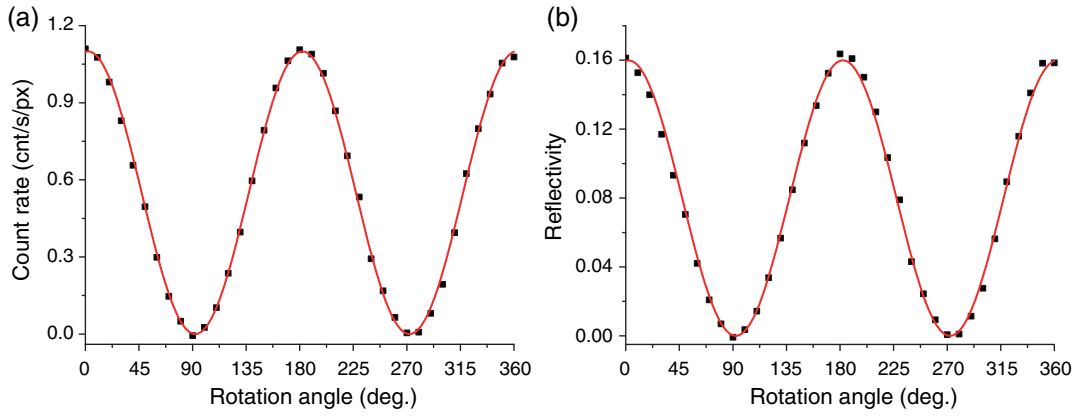


**Fig. 5** Results of the soft x-ray polarimetry experiment on a Co/C multilayer. (a) CCD count rate per pixel as a function of the rotation angle and a sine-wave fitting curve. (b) Reflectivity of the Co/C multilayer sample as a function of the rotation angle and a sine-wave fitting curve.

the CCD count rates are almost zero, which implies that the combination of the soft x-ray light source and the multilayer polarizer produces nearly 100% linearly polarized x-rays. Additionally, the linearly polarized light can be rotated from 0 deg to 360 deg in the plane perpendicular to the beam-propagation direction. The count rates, as given in Figs. 4(a) and 5(a), represent the intensity of the incident and reflected beams, respectively. The ratio of the reflected intensity to the incident intensity is the reflectivity of the Co/C multilayer sample, which is shown in Fig. 5(b). It can be seen that the maximum reflectivity is 0.16 for s-polarized light, which is close to the estimated reflectivity of 0.18 according to our previous experimental results.<sup>7</sup> For p-polarized light, the minimum reflectivity is almost zero, which is in agreement with the theoretical prediction. It is noted that the incident and reflected beam intensities were not measured in the same experimental run, because the CCD detector has to be moved to a different flange. But for both measurements, the beam current of the light source was set at  $0.4 \pm 0.001$  mA. It was also checked that the incident-beam intensity variation was less than 2% when using this beam current.

### 3.4 Discussion on the Requirements on Experimental Errors

The figure of merit of a flight polarimeter is characterized by the minimum detectable polarization (MDP),<sup>20</sup> which is defined at a 99% confidence level as:

$$\text{MDP} = \frac{4.29}{\mu R_s} \sqrt{\frac{R_s + R_B}{T}}. \quad (1)$$

Here,  $\mu$  is the modulation factor of the polarimeter for a fully polarized source.  $R_s$ ,  $R_B$ , and  $T$  represent the source, background count rates, and the exposure time, respectively. For the LAMP proposal, 46 bright sources with MDP below 10% were considered as the potential targets using the modulation factor  $\mu \sim 88.7\%$ , the background count rate of  $1.47 \times 10^{-3}$  counts/s, and the expected signal count rates with an exposure time of  $10^6$  s as given in Table 1 of Ref. 5. Based on Eq. (1), the requirement on the polarization measurement errors can also be evaluated in order to fulfill the main missions of the LAMP proposal. The evaluation principal is

that the majority of the potential targets should still be detectable with the MDP below 10% after taking the experimental errors into account. For simplicity, let us assume that the modulation factor  $\mu$  and the reflectivity of  $R$  have the same RRMSE of  $\eta$ . Based on the Gaussian distribution confidence intervals principle, the measured  $\mu$  and  $R$  would have 99% probability lying within the confidence intervals of  $[\mu - 2.58 \mu \eta, \mu + 2.58 \mu \eta]$  and  $[R - 2.58 R \eta, R + 2.58 R \eta]$ , respectively. Using the lower limit value  $\mu - 2.58 \mu \eta$  and  $R - 2.58 R \eta$ , we calculated the MDP for all the sources given in Ref. 5 with different  $\eta$ . It should be mentioned that  $R_s$  is replaced by  $R_s - 2.58 R_s \eta$  in this calculation since  $R_s$  is proportional to  $R$ . It is found that, when the RRMSE  $\eta$  equals to 10%, there are still 39 potential bright sources targets having MDP below 10%. Since the majority of the potential targets are still detectable for the LAMP proposal, the RRMSE less than 10% is considered as an acceptable experimental error for the polarization measurement using this polarimeter.

In our measurement, there are several factors which give rise in errors for the polarization and reflectivity measurement. The main systematic error is caused by the fluctuation of the incident beam flux during rotating the light source, which has the RRMSE of 4.5% as mentioned in Sec. 3.2. This error is mainly caused by the misalignment between the rotation axis of the light-source chamber and the optical axis of the beamline. In addition, the slight shift and vibration of the polarizer mirror during rotation may also contribute partly to the flux fluctuation. By combining this systemic error with the stability error of the incident beam intensity (RRMSE = 2% as mentioned in Sec. 3.3), the total error for the incident beam intensity is about 4.9%. For the reflectivity measurement as shown in Fig. 5(b), it is determined by the reflected beam intensity  $I_R$  normalized to the incident beam intensity  $I_0$ , namely  $R = I_R/I_0$ . Since the reflected and incident beam intensities were not measured simultaneously, the fluctuations for both beams cannot cancel each other out. Therefore, the experimental error for the reflected beam intensity measurement should also be considered with the same RRMSE of 4.9% as the incident beam. By combining all errors together, the experimental error for the reflectivity is estimated to be about 6.9% (RRMSE). For the modulation factor, the measurement error is estimated using the equation  $\mu = \frac{R_s - R_p}{R_s + R_p}$ , where  $R_s$  and  $R_p$  are the reflectivity for the s- and p-polarized lights, namely

the maximum and the minimum reflectivity in Fig. 5(b). According to the error propagation, the RRMSE for  $\mu$  at the Brewster angle is estimated to be less than 2% because of the very small ratio of  $R_p/R_s$ . So, all the experimental errors for the reflectivity and the polarization measurements meet the requirements of RRMSE of 10% for the LAMP proposal. In our polarimeter setup, there are some other minor error sources, such as the incident beam position shift, the incidence angle variation, nonuniform response of the CCD detector, and statistic errors for collected counts, which are small and not considered in this paper.

## 4 Conclusion

This paper described the designed structure and alignment method for a table-top soft x-ray polarimetry setup, which is planned to test the polarization properties of mirrors. This setup can generate linearly polarized soft x-ray light that is rotatable around the beam-propagation direction. The beam divergence and the incident-beam intensity/position stability were measured using this setup. In addition, a polarimetry test on a Co/C multilayer sample was performed. According to the experimental results, the performance of the soft x-ray polarimetry setup is summarized as follows:

1. The FWHM of the x-ray spot diameter is  $\sim 0.43$  mm, and the FWHM of the divergence of polarized x-rays is  $\sim 0.08$  deg.
2. The intensity variation of the polarized x-ray beam is less than 4.5% (RRMSE), and the polarized x-ray spot in the detector varies by  $\pm 0.28$  mm in the horizontal direction and  $\pm 0.55$  mm in the vertical direction when rotating the source chamber.
3. This setup can produce nearly 100% rotatable linearly polarized x-rays, and the reflectivity for the sample mirror can also be approximately determined.

Presently, this system can only be used to test the polarization property and reflectivity for small and flat mirrors at an incidence angle of 45 deg. In the near future, a multiaxis goniometer is planned to be set up to perform  $\theta - 2\theta$  reflectivity measurements for large-scale samples.

## Acknowledgments

This work was supported by the National Key Research and Development Program of China (2016YFA0401304) and National Natural Science Foundation of China (NSFC) (Grant Nos. 11375130 and 61621001).

## References

1. W. Jaffe et al., "The central dusty torus in the active nucleus of NGC 1068," *Nature* **429**(6987), 47–49 (2004).
2. A. L. McNamara et al., "X-ray polarization in relativistic jets," *Mon. Not. R. Astron. Soc.* **395**(3), 1507–1514 (2009).
3. H. L. Marshall et al., "Realistic, inexpensive, soft x-ray polarimeter and the potential scientific return," *Proc. SPIE* **4843**, 360–371 (2003).
4. S. S. Panini et al., "Multilayer mirror-based soft x-ray polarimeter for astronomical observations," *J. Astron. Telesc. Instrum. Syst.* **4**(1), 011002 (2017).
5. S. Rui et al., "LAMP: a micro-satellite based soft x-ray polarimeter for astrophysics," *Proc. SPIE* **9601**, 96010I (2015).

6. M. W. Wen et al., "High efficiency carbon-based multilayers for LAMP at 250 eV," *Proc. SPIE* **9603**, 96031A (2015).
7. M. W. Wen et al., "Improvement of interface structure and polarization performance of Co/C multilayers," *Opt. Express* **24**(24), 27166–27176 (2016).
8. S. Nannarone et al., "The BEAR beamline at Elettra," *AIP Conf. Proc.* **705**, 450–453 (2004).
9. F. Schäfers et al., "Soft-x-ray polarimeter with multilayer optics: complete analysis of the polarization state of light," *Appl. Opt.* **38**(19), 4074–4088 (1999).
10. J. I. Larruquet et al., "GOLD's coating and testing facilities for ISSIS-WSO," *Astrophys. Space Sci.* **335**, 305–309 (2011).
11. D. L. Windt and W. K. Waskiewicz, "Soft x-ray reflectometry of multilayer coatings using a laser-plasma source," *Proc. SPIE* **1547**, 144–158 (1991).
12. D. N. Gurgew et al., "X-ray reflectometer for single layer and multilayer coating characterization at 8 keV: an interlaboratory study," *Rev. Sci. Instrum.* **87**, 104501 (2016).
13. L. Loyer et al., "Laboratory LPP EUV reflectometer working with non-polarized radiation," *Appl. Surf. Sci.* **252**, 57–60 (2005).
14. S. Nakayama et al., "Soft x-ray reflectometer with a laser-produced plasma source," *Phys. Scr.* **41**, 754–757 (1990).
15. H. L. Marshall et al., "Progress toward a soft x-ray polarimeter," *Proc. SPIE* **8861**, 88611D (2013).
16. S. N. T. Heine et al., "Laboratory progress in soft x-ray polarimetry," *Proc. SPIE* **10399**, 1039916 (2017).
17. H. L. Marshall et al., "The use of laterally graded multilayer mirrors for soft x-ray polarimetry," *Proc. SPIE* **9603**, 960319 (2015).
18. J. E. Manson, "Model 2 ultrasoft x-ray source installation and operating instructions," Austin Instruments Inc. (1988).
19. D. L. Windt, "IMD-software for modeling the optical properties of multilayer films," *Comp. Phys.* **12**, 360–370 (1998).
20. M. C. Weisskopf et al., "On understanding the figures of merit for detection and measurement of x-ray polarization," *Proc. SPIE* **7732**, 77320E (2010).

**Wenbin Li** is a professor at the School of Physics Science and Engineering of Tongji University. He received his BS degree in physics from Anhui Normal University in 1995, and his PhD in physics from the University of Science and Technology of China in 2004. His current research interests include x-ray multilayer mirrors, soft x-ray polarimetry, EUV/x-ray reflectometer, and EUV/x-ray damage.

**Yujie Xing** is a graduate student from Tongji University. He received his BS degree in mechanical from Jiangsu University of Science and Technology in 2015. He received his MS degree in optics from Tongji University in 2018. His research interests are soft x-ray polarimetry and x-ray instruments.

**Yue Yu** is currently a graduate student from Tongji University. She received her BS degree from Ocean University of China in 2017. Her current research interests are soft x-ray polarimetry and x-ray optical system.

**Mingwu Wen** is a graduate student from Tongji University. He received his BS degree and PhD in optics from Tongji University in 2012 and 2017, respectively. His research interests include grazing-angle x-ray scattering, indirect glass slumping technology, and soft x-ray multilayer polarizer.

**Chun Xie** is an associate professor at Tongji University. She received her MS degree in mechanical engineering from Changchun University of Technology in 1989 and her PhD in mechanical manufacturing and automation from Tongji University in 2013. Her current research interests include precision machinery and optical instruments in EUV, soft x-ray, and x-ray region.

**Qiushi Huang** is an associate professor at the School of Physics Science and Engineering of Tongji University. He received his MS degree in optics engineering and PhD in optics from Tongji University, in 2009 and 2012, respectively. He is the author of over 50 journal papers and his current research interests include EUV and x-ray multilayers optics, grating optics, and mirror fabrication technology.

**Zhong Zhang** is a professor at the School of Physics Science and Engineering of Tongji University. He received his PhD in condensed matter physics from Tongji University in 2006. His current research interests include x-ray and neutron optical coating, neutron optics, and detectors, as well as x-ray optical systems.

**Shengzhen Yi** is currently an assistant professor at the School of Physics Science and Engineering of Tongji University. He received his BS and MS degrees in physics and PhD in optics from Tongji University in 2006, 2009, and 2012, respectively. His current research

interests focus on the x-ray imaging optics for laser-plasma diagnostics.

**Zhanshan Wang** is a SPIE fellow and a professor at Tongji University. He received his MS degree in optics from Changchun Institute of Optics and Fine Mechanics in 1988 and his PhD in optics from Shanghai Institute of Optics and Fine Mechanics in 1996. He is the author of more than 150 journal papers. His current research interests include soft x-ray sources, optics in EUV, soft x-ray, and x-ray region, optical coatings for lasers and optical systems.